JOURNAL OF SOLID STATE CHEMISTRY 106, 111–119 (1993)

Weak Ferromagnetic Behavior of the Manganese Alkylphosphonate Hydrates $MnC_nH_{2n+1}PO_3 \cdot H_2O$, $n = 1–4$

SIMON G. CARLING AND PETER DAY*

Davy–Faraday Research Laboratory, Royal Institution of Great Britain, 21, Albemarle Street, London W1X 4BS, United Kingdom

DICK VISSER

Physics Department, Loughborough University of Technology, Loughborough LE11 3TU, United Kingdom

AND R. K. KREMER

Max Planck Institut für Festkörperforschung, Stuttgart, Germany

Received December 4, 1992; accepted December 23, 1992

IN HONOR OF SIR JOHN MEURIG THOMAS ON HIS 60TH BIRTHDAY

Alkylphosphonates $MnC_nH_{2n+1}PO_3 \cdot H_2O$, $n = 1–4$, were prepared from aqueous solution and studied using bulk magnetic techniques. Orthorhombic unit cell parameters have been determined from X-ray powder data. The compounds form a homologous series, apparently analogous to the inorganic phosphates $M^{I}M^{II}PO_4 \cdot H_2O$, consisting of distorted MO_6 octahedra cross-linked into sheets by phosphonate oxygens, the sheets being separated by alkyl chains. All four compounds are canted antiferromagnets, with ordering temperatures in the range 14.8–15.1 K. The magnitude of the spin canting varies significantly with the length of the alkyl chain; there is also an apparent alternation in T_N with odd and even chain lengths.

Introduction

Ionic compounds of the transition elements exhibiting a finite spontaneous (zero-field) magnetization are very few and far between: the overwhelming majority of magnetic materials are metallic. The challenge of seeking new nonmetallic ferromagnets is therefore an entirely appropriate one to be accepted by the solid state synthetic chemist. Physical mechanisms of ferromagnetic exchange coupling between localized moments are based on the notion of "orthogonal magnetic orbitals" (*1*), a situation that is very difficult to achieve in a three-dimensionally continuous lattice. We showed some time ago (*2*) that in two dimensions a cooperative Jahn–Teller lattice distortion provided a suitable means of creating "orbital ordering," such that singly occupied 3*d* orbitals on a given metal ion were rendered orthogonal to the corresponding ones on all the nearest neighbor ions. The resulting series A_2CrX_4 (A representing a wide range of monopositive organic and inorganic cations and X a halide ion) are ferromagnets with Curie temperatures between 30 and 60 K (*3*). Among discrete molecular oligomers, the same principle was also demonstrated by Kahn and his colleagues (*4*) in

* To whom correspondence should be addressed.

0022-4596/93 $5.00

coordination complexes of VO^{2+} and Cu^{2+} (d^1, d^9), but other examples have proved elusive.

Given the difficulty of engineering near-neighbor ferromagnetic exchange in the absence of conduction electrons, it is appropriate to seek alternative strategies for inducing finite zero-field magnetization. One route lies in exploiting ferrimagnetism; that is, in making compounds containing two different metal ions that interact antiferromagnetically but that do not cancel, having unequal moments. Again, this approach has been implemented successfully by Kahn and his colleagues (*5*) with respect to molecular magnetic materials while, in the conventional inorganic solid state, such compounds as the rare-earth iron garnets have been widely studied for many years (*6*). Applications include magnetooptic "bubble" memory devices.

A third strategy, less exploited than the other two, consists in synthesizing lattices containing only one kind of magnetic ion, in which, because of competition with single-ion anisotropy induced by a low-symmetry ligand field and second-order spin–orbit coupling, the moments on neighboring ions are not precisely antiparallel. This is called canted antiferromagnetism or (because the resultant of two vectors that are nearly, but not quite, antiparallel is a small vector at right angles) weak ferromagnetism. An example that was much studied more than 20 years ago as a magnetooptic memory medium is $FeBO_3$ (*7, 8*). We have implemented such a strategy, to prepare organic–inorganic layer compounds having a spontaneous magnetization by synthesizing a series of alkylphosphonate salts of 3*d* elements. Our aim has been to discover how the canted moment varies with the length of the alkyl sidechain and the metal ion. In this paper we report on a series of Mn^{II} alkylphosphonates in which the spin canting proves to be surprisingly sensitive to the nature of the organic substituent.

The series of phosphates $M^{I}M^{II}PO_4 \cdot H_2O$ (M^{I} = K, NH_4; M^{II} = Mn, Fe, Co, Ni) were reported by Bassett and Bedwell in 1933 (*9*). The crystal structure of $NH_4CoPO_4 \cdot H_2O$ was determined in 1968 (*10*) and the unit cell parameters of the remaining compounds were reported in the same year (*11*) and the unit cell parameters of the remaining compounds were reported in the same year (*11*). All these materials crystallize in the orthorhombic space group $Pmn2_1$. The structure consists of approximately square planar sheets of M^{II} ions, coordinated in a severely distorted octahedron by five phosphate oxygens and one water molecule, separated by the monovalent cation. The point symmetry corresponding to the symmetry of the space group is C_{2v}.

An analogous series of phosphonate compounds exists, in which the metal-containing layers are separated by organic, rather than inorganic material. Cunningham *et al.* (*12*) synthesized the phenylphosphonates $M^{II}PhPO_3 \cdot H_2O$ for M^{II} = Mg, Mn, Fe, Co, and Ni. Magnetic measurements in the temperature range 90–300 K showed Curie–Weiss behavior characteristic of antiferromagnetic interaction for the Mn and Fe compounds. Mallouk and co-workers have reported the synthesis of straight-chain alkylphosphonates $MgC_nH_{(2n+1)}PO_3 \cdot H_2O$ for n = 1–12 (*13*) and also determined the crystal structure of $MnPhPO_3 \cdot H_2O$ (*14*). All these compounds crystallize in space group $Pmn2_1$, and the structure of the metal-containing layer is the same as that found for $NH_4CoPO_4 \cdot H_2O$.

$NH_4FePO_4 \cdot H_2O$ was found by Greedan *et al.* to be weakly ferromagnetic (*15*). Our own work shows that the manganese compounds $NH_4MnPO_4 \cdot H_2O$ and $KMnPO_4 \cdot H_2O$ are also weakly ferromagnetic, though to a lesser extent, and we have used powder neutron diffraction to determine the underlying antiferromagneticstructure of all three of these compounds (*16, 17*). We report here the extension of these studies to the alkylphosphonates $MnC_nH_{2n+1}PO_3 \cdot H_2O$, where n = 1–4.

TABLE I

ELEMENTAL ANALYSES OF THE MANGANESE ALKYLPHOSPHONATE HYDRATES

	Percentages by mass					
	Mn		C		H	
R	Obs	Calc	Obs	Calc	Obs	Calc
CH_3	32.88	32.90	7.10	7.19	3.00	3.02
C_2H_5	29.71	30.36	13.25	13.27	3.79	3.90
C_3H_7	25.88	28.17	17.31	18.48	4.50	4.65
C_4H_9	26.84	26.28	22.01	22.98	5.42	5.30

Experimental Details

Synthesis of Compounds

Samples were prepared by a method similar to that described in Ref. (*13*). Alkylphosphonic acids were supplied by Lancaster Synthesis, except for propylphosphonic acid, which was supplied by Aldrich. "Analar" $MnCl_2 \cdot 4H_2O$ was supplied by BDH. All compounds were used as supplied, without further purification. Deionized water was produced using a Fison's Fionmatic 400.

A solution of approximately 1 g of alkylphosphonic acid in 30–40 ml of deionized water was adjusted to a pH of between 7 and 8 with approximately 0.1 M KOH. An equimolar amount of $MnCl_2 \cdot 4H_2O$ was dissolved in approximately 10 ml of water and added to the alkylphosphonate solution. The resulting dense white precipitate was heated under reflux for 48–72 hr at 85 ± 5°C to improve the crystallinity of the product, then filtered off, washed with deionized water, and dried *in vacuo*.

Characterization of Compounds

Elemental analysis. Elemental analyses were carried out by the Microanalysis Service of the Inorganic Chemistry Laboratory, Oxford. Metals were assayed by atomic absorption spectroscopy, while carbon, nitrogen, and hydrogen contents were determined by combustion. The results of these analyses are presented in Table I.

Powder X-ray diffraction. Powder X-ray profiles were recorded using Cu$K\alpha$ radiation from a Phillips PW1723 X-ray generator controlled by a PW1710 diffractometer control unit. Samples were mounted on aluminum plates in a flat geometry, which gives rise to a strong preferred orientation, with the stacking axis perpendicular to the plate. Unit cell parameters were refined from unambiguously indexed lines in the profile using the Refcell program written by Cockcroft (*18*) or the Cellref program based on the methods described by Rollet (*19*). The numbers of observed lines between 10° and 80° 2θ which could be unambiguously indexed were as follows: for $MnCH_3PO_3 \cdot H_2O$ 18 lines, for $MnC_2H_5PO_3 \cdot H_2O$ 8 lines, for $MnC_3H_7PO_3 \cdot H_2O$ 16 lines, and for $MnC_4H_9PO_3 \cdot H_2O$ 10 lines (of which 6 were (0 *k* 0) reflections). Results of these refinements are given in Table II. The unit cell parameters determined here for $MnCH_3PO_3 \cdot H_2O$ are in good agreement with those reported in Ref. (*14*).

Magnetic Measurements

The magnetic data presented here were collected on a Cryogenics S600 SQUID magnetometer at the Inorganic Chemistry Laboratory, Oxford, and a Quantum Design MPMS5 SQUID magnetometer at the Max Planck Institut Festkorperforschung, Stuttgart. The sample under investigation was loaded into a quartz bucket suspended on a copper wire in the former case, and a gelatin capsule in a plastic drinking straw in the latter. Samples were first cooled in the absence of an applied field; the susceptibility

TABLE II

UNIT CELL PARAMETERS OF $MnRPO_3 \cdot H_2O$

R	*a*/Å	*b*/Å	*c*/Å
CH_3	5.819(2)	8.818(2)	4.897(2)
C_2H_5	5.83(6)	10.24(6)	4.87(8)
C_3H_7	5.84(4)	11.71(2)	4.91(2)
C_4H_9	5.84(4)	14.72(2)	4.91(8)

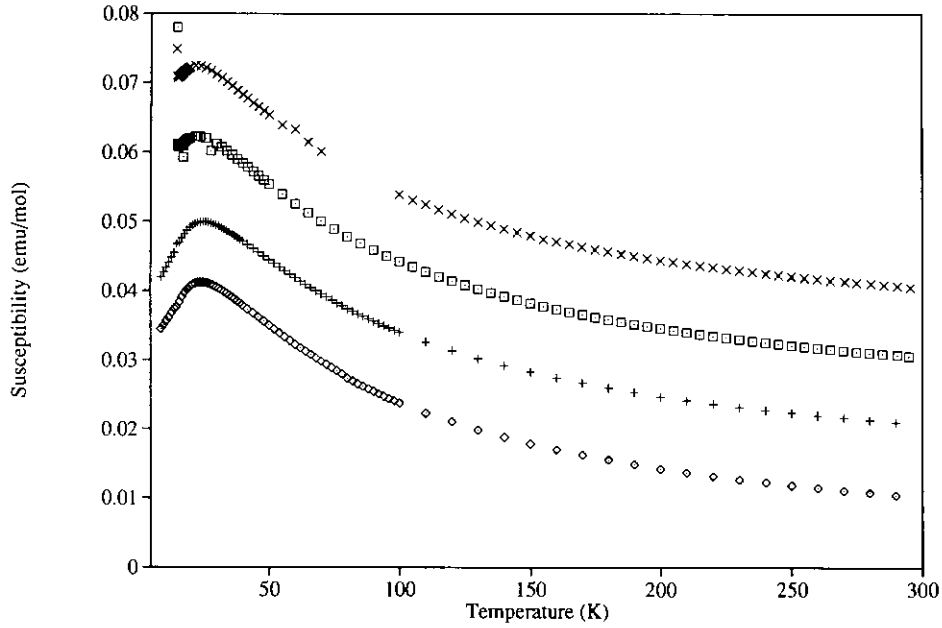

FIG. 1. Susceptibilities of the alkylphosphonates $MnC_nH_{2n+1}PO_3 \cdot H_2O$ in a field of 100 G. $n = 1$, (◇); $n = 2$, (+); $n = 3$, (□); $n = 4$, (×). Susceptibility scale is shown for $n = 1$; other chain lengths are offset by increments of 0.01 emu mol^{-1}.

between 5 K and 300 K was then measured on warming in a field of 100 G, and on recooling through the ordering transition in the same field. In the case of $MnCH_3PO_3 \cdot H_2O$ the susceptibility was measured on warming in 100 G after cooling in zero field and in the residual field of the magnet (approximately 100 G) after cooling in 1.0 kG. Corrections for diamagnetism of the sample holder were applied to the measured moment, and the resulting susceptibilities were corrected for sample diamagnetism estimated from values given in Refs. (*20, 21*).

Results

Figure 1 shows the susceptibilities of the compounds $MnC_nH_{2n+1}PO_3 \cdot H_2O$ from 5 to 300 K. Above ~80 K the data show good agreement with the Curie–Weiss law. The values of the Curie and Weiss constants determined from this data are shown in Table III, along with the effective moments, μ_{eff}, calculated from the Curie constants. The values of μ_{eff} are significantly lower than the "spin-only" value of 5.92 μ_B for a spin $\frac{5}{2}$ ion, presumably due to the effects of covalency. Below ~80 K, short range order causes deviations from this simple model, and all four compounds show the broad maximum characteristic of two dimensional antiferromagnetism.

Figure 2 shows the zero-field cooled (zfc) susceptibility of $MnCH_3PO_3 \cdot H_2O$, along with the moment (not to scale) measured in the remanent field of the magnet after cooling in 1.0 kG. The weak-ferromagnetic moment is clearly very small, being smaller than the antiferromagnetic moment induced by the remanent field, but the sharp decrease in moment at 14.87(5) K shows that some canting does occur. Note that there is only a slight inflection in the susceptibility curve at T_N. Figures 3–5 show the susceptibilities of the C_2, C_3, and C_4 phosphonates, respectively, both warming in 100 G after cooling in zero field and on subsequent cool-

TABLE III

MAGNETIC PARAMETERS OF THE ALKYLPHOSPHONATES $MnC_nH_{2n+1}PO_3 \cdot H_2O$

R	C/cgs	θ/K	μ_{eff}/μ_B	$T(\chi_{max})$/K	$\frac{\lvert J \rvert}{k}$/K	μ_{ferro}/μ_B	α/°
CH_3	3.56(1)	−48.9(7)	5.36(1)	24.3(2)	1.35(2)	—	—
C_2H_5	3.84(2)	−59.7(7)	5.57(1)	25.0(2)	1.39(2)	0.010(1)	0.10(1)
C_3H_7	3.68(1)	−51.7(7)	5.45(1)	22.4(4)	1.24(4)	0.143(1)	1.50(1)
C_4H_9	3.68(1)	−54.4(9)	5.45(1)	22.4(3)	1.24(3)	0.278(1)	2.92(1)

ing in that field. $MnC_2H_5PO_3 \cdot H_2O$ shows a sharp cusp in its zfc susceptibility at T_N = 15.10(5) K, and on cooling through the transition develops a moment significantly greater than was found in $MnCH_3PO_3 \cdot H_2O$. Both $MnC_3H_7PO_3 \cdot H_2O$ and $MnC_4H_9PO_3 \cdot H_2O$ show a net magnetic moment when cooled through T_N in zero field. The Néel temperatures of these compounds are 14.90(5) and 15.01(5) K respectively. In both compounds the weak ferromagnetic moment increases on recooling in the field, more so in the case of $MnC_4H_9PO_3 \cdot H_2O$ than in that of $MnC_3H_7PO_3 \cdot H_2O$. This is ascribed to the alignment of magnetic domains by the applied field.

The weak ferromagnetic moments can be estimated from the susceptibility data for the latter three compounds if one assumes that the antiferromagnetic contribution to the susceptibilities of $MnC_3H_7PO_3 \cdot H_2O$ and $MnC_4H_9PO_3 \cdot H_2O$ below T_N is the same as that measured for $MnC_2H_5PO_3 \cdot H_2O$. For $MnCH_3PO_3 \cdot H_2O$ the moment is too small to be estimated with any accuracy. The ferromagnetic moments are shown in Table III, and the variation of Néel temperature is shown graphically in Fig. 6.

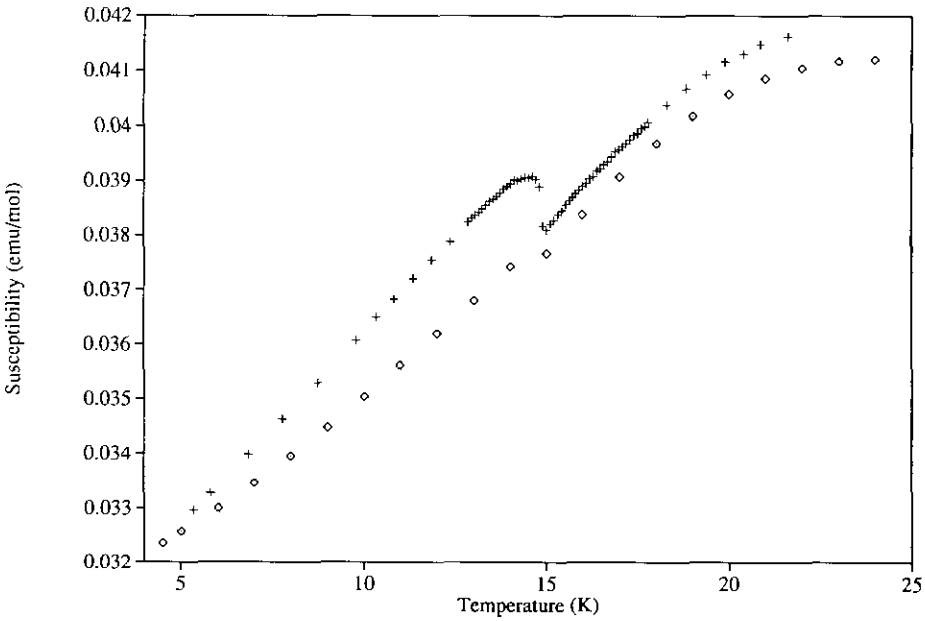

FIG. 2. $MnCH_3PO_3 \cdot H_2O$: zero field cooled susceptibility in 100 G (◇), and remanent field moment after cooling in 1 kG (+).

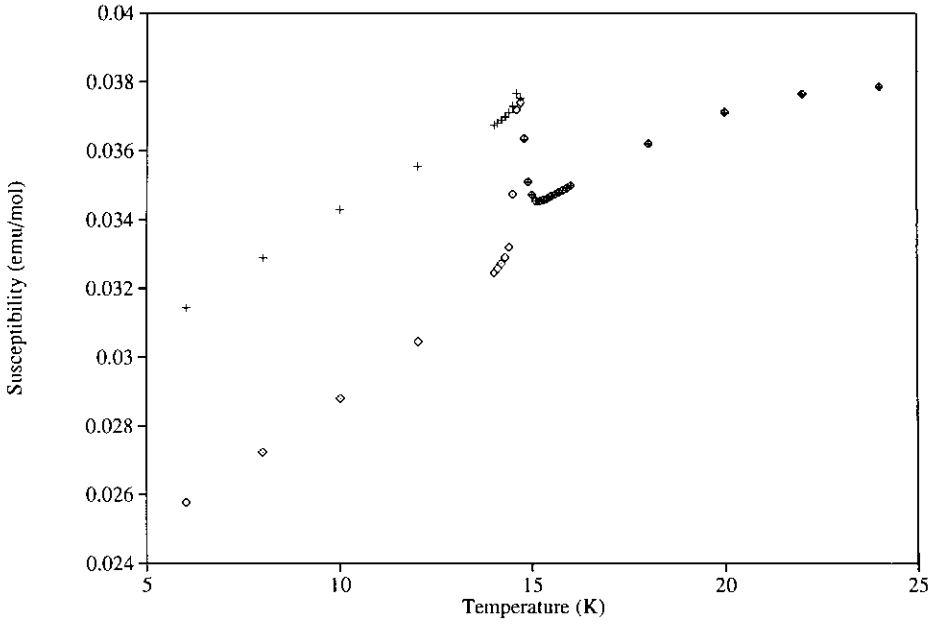

FIG. 3. $MnC_2H_5PO_3 \cdot H_2O$: zero field cooled susceptibility in 100 G (◇), and susceptibility cooling in 100 G (+).

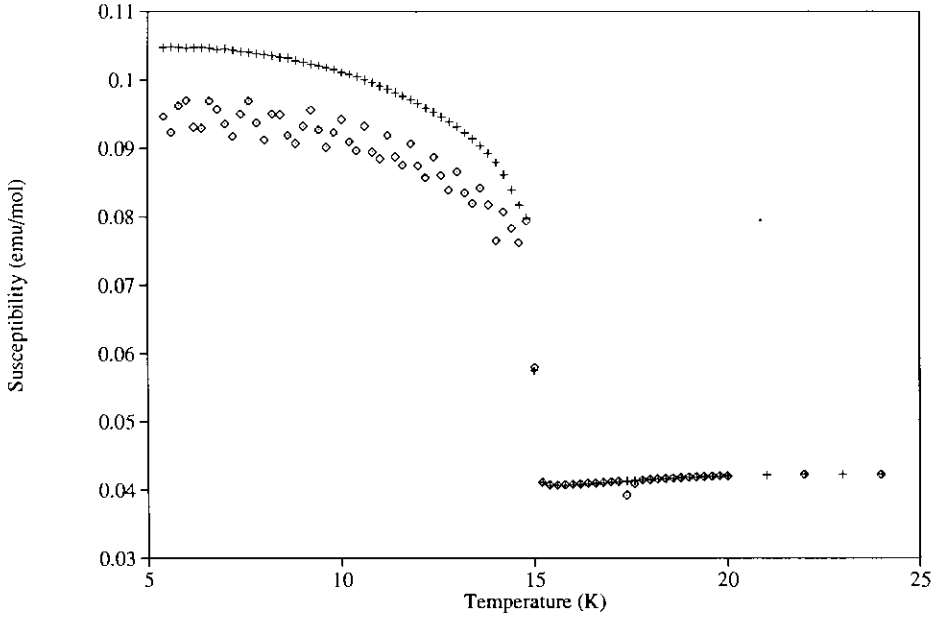

FIG. 4. $MnC_3H_7PO_3 \cdot H_2O$: zero field cooled susceptibility in 100 G (◇), and susceptibility cooling in 100 G (+).

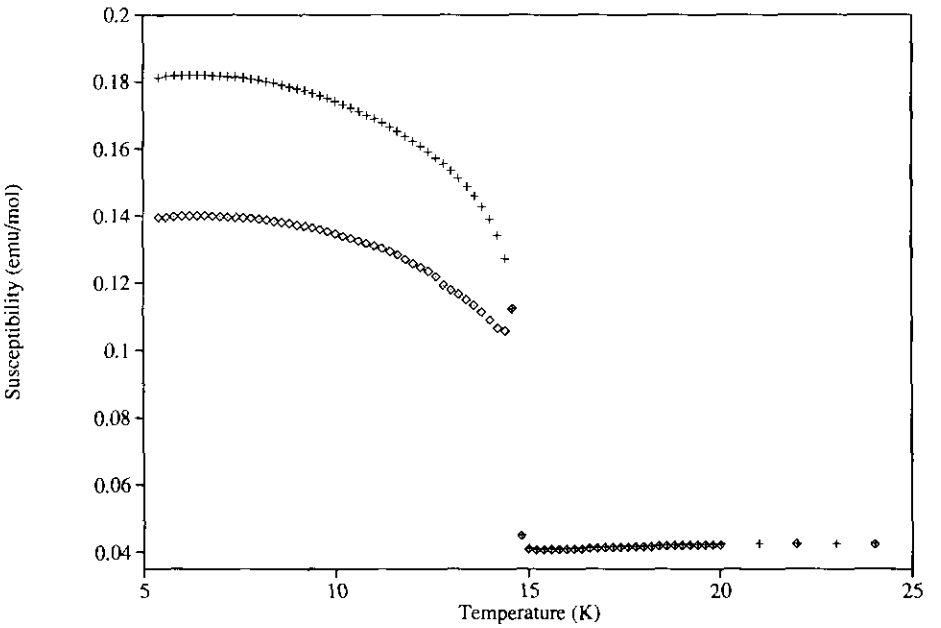

FIG. 5. $MnC_4H_9PO_3 \cdot H_2O$: zero field cooled susceptibility in 100 G (◇), and susceptibility cooling in 100 G (+).

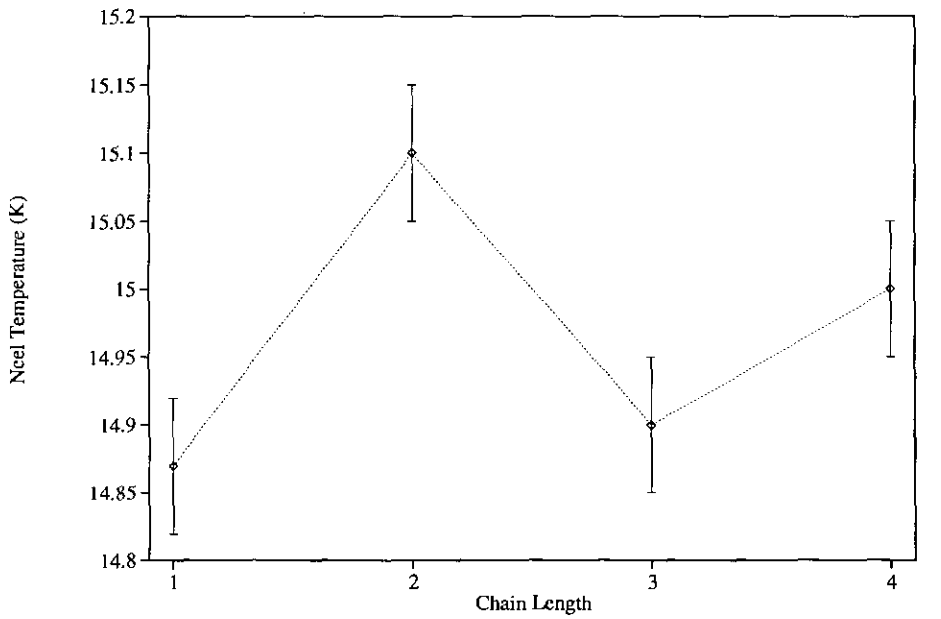

FIG. 6. Variation of ordering temperature, T_N, with chain length n. The dashed line is a guide to the eye.

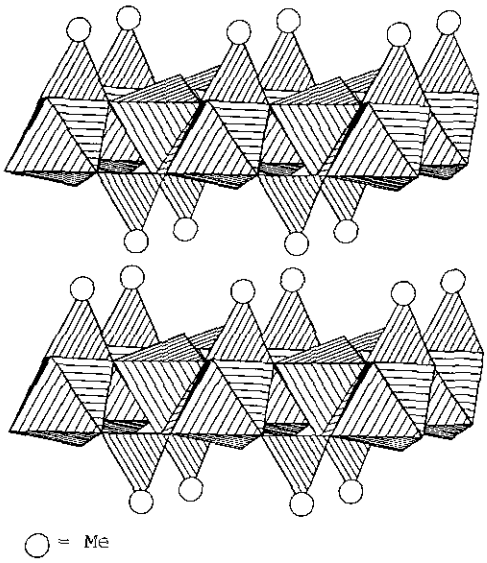

FIG. 7. Suggested structure for $MnCH_3PO_3 \cdot H_2O$.

Discussion

Although the precise atomic coordinates of these materials are not yet known, the unit cell parameters shown in Table II show that the inorganic layers are almost identical to those in the ammonium and potassium salts, and there is no evidence of variation with alkyl chain length. The *c*-axis parameter is the same (within experimental error) as that found in $NH_4MnPO_4 \cdot H_2O$ and $KMnPO_4 \cdot H_2O$ (*16*, *17*); while there is a slight increase in *a*, this is no larger than the increase found between $KMnPO_4 \cdot H_2O$ and $NH_4MnPO_4 \cdot H_2O$. It is probable that the nature of the layer structure of these materials is essentially the same as has been determined for those compounds and $MnPhPO_3 \cdot H_2O$. The marked variation in canting with increasing chain length must therefore be due to a very subtle change in structure, the nature of which remains to be determined. In the phosphate compounds, the P–O bond not involved in coordinating manganese lies in the *bc* plane at a slight angle to the *b* axis. The most probable structure for the phosphonate compounds would replace this P–O bond with a P–C bond, as illustrated for $MnCH_3PO_3 \cdot H_2O$ in Fig. 7, and it is therefore possible that the packing of the longer chains exerts a torque on the phosphonate group, leading to a change in the distortion of the MO_6 octahedron. The apparent alternation of T_N with odd and even chain lengths would seem to support this hypothesis, since successive C–C bonds alternate in angle to the stacking axis as a consequence of the *trans* nature of the alkyl chains; however, study of further compounds with longer alkyl chains will be required to confirm the nature of this effect.

The position of the maximum in the antiferromagnetic susceptibility, $T(\chi_{max})$, is directly related to the intraplanar exchange constant, *J* (*23*). The relationship for a square planar, spin $\frac{5}{2}$, Heisenberg antiferromagnet is

$$\tau_m = \frac{k_B T(\chi_{max})}{|J|S(S+1)} = 2.06 \pm 0.03$$

Values of $T(\chi_{max})$, and the corresponding value of $|J|$ for a square planar Heisenberg antiferromagnet with $S = \frac{5}{2}$ are also given in Table III.

The symmetry of space group $Pmn2_1$ is sufficiently low that the antisymmetric exchange proposed by Moriya (*22*) to account for weak ferromagnetism can occur. The exchange, which operates in addition to the isotropic Heisenberg exchange, is described on a microscopic level as

$$\hat{\mathcal{H}}_{aniso} = \mathbf{d} \cdot [\mathbf{s}_1 \times \mathbf{s}_2].$$

This antisymmetric exchange derives from the anisotropic spin interaction, which can be described as the sum of symmetric and antisymmetric components,

$$V_{1,2} = \mathbf{s}_1 \cdot \mathbf{K}_S \cdot \mathbf{s}_2 + \mathbf{s}_1 \cdot \mathbf{K}_A \cdot \mathbf{s}_2,$$

where the symmetric and antisymmetric tensors $\mathbf{K}_S$ and $\mathbf{K}_A$ are approximated by

$$\mathbf{K}_S \sim \left(\frac{\lambda}{\Delta}\right)^2 J \sim \left(\frac{\Delta g}{g}\right)^2 J$$

and

$$\mathbf{K}_A \sim \left(\frac{\lambda}{\Delta}\right) J \sim \left(\frac{\Delta g}{g}\right) J$$

respectively, when λ is the spin–orbit coupling, Δ the ligand field splitting, and $\Delta g = g - 2$. Only the antisymmetric component can cause spin canting. Since the ground state of Mn^{2+} is $^6S_{5/2}$, the spin–orbit coupling is very small; the low site symmetry, however, induces anisotropy in the g-tensor.

A measure of the canting angle, α, of the Mn^{2+} spins can be obtained by comparing the ferromagnetic moments determined above with the paramagnetic moments extracted from fitting the high temperature susceptibilities to the Curie–Weiss law:

$$\alpha = \sin^{-1}\left(\frac{\mu_{\text{ferro}}}{\mu_{\text{eff}}}\right)$$

The values thus calculated are shown in Table III. The absolute magnitude of the ferromagnetic moment is of course reduced by domain effects, and these estimates of the canting angle should therefore be regarded as lower limits.

Moriya also describes constraints on the direction of the vector **d** imposed by crystal symmetry (*22*). In the case of the compounds described here, the symmetry operation which relates the metal centers of the two sublattices is the $(\frac{1}{2}\ 0\ \frac{1}{2})$ glide plane, and **d** is therefore constrained to lie parallel to this plane. This is compatible with our magnetic structure determination for the inorganic analogues of these materials (*17*) using Bertaut's method of irreducible representations (*24*) from which we concluded that the weak ferromagnetic moment must lie parallel to the crystallographic c-axis.

Acknowledgments

The authors acknowledge the assistance of E. Brücher of the Max Planck Institut für Festkörperforschung, Stuttgart, in making magnetic measurements, and funding from the U.K. Science and Engineering Research Council for funding under the 21st Century Materials Initiative.

References

1. A. Ginsberg, *Inorg. Chim. Acta Rev.* **5,** 45 (1971).
2. P. Day, A. K. Gregson, D. H. Leech, and M. J. Fair, *J. Chem. Soc. Dalton Trans.*, 1306 (1975).
3. P. Day, *J. Magn. Magn. Mater.* **54–57,** 1442 (1986).
4. O. Kahn, J. Galy, Y. Journaux, J. Jaud, and I. Morganstern-Badarau, *J. Am. Chem. Soc.* **104,** 2165 (1982).
5. O. Kahn, *Philos. Trans. R. London Ser. A* **330,** 123 (1990).
6. K. J. Standley, "Oxide Magnetic Materials," Oxford Univ. Press, Oxford (1962).
7. J. C. Joubert, T. Shirk, W. B. White, and R. Roy, *Mater. Res. Bull.* **3,** 671 (1968).
8. A. J. Kurtzig, R. Wolfe, R. C. LeCraw, and J. W. Nielsen, *Appl. Phys. Lett.* **14,** 350 (1969).
9. H. Bassett and W. L. Bedwell, *J. Chem. Soc.*, 854 (1933).
10. D. Tranqui, A. Durif, J.-C. Guitel, and M. T. Averbuch-Pouchot, *Bull. Soc. Fr. Miner. Cristallogr.* **91,** 10 (1968).
11. A. Durif and M. T. Averbuch-Pouchot. *Bull. Soc. Fr. Miner. Cristallogr.* **91,** 495 (1968).
12. D. Cunningham, P. J. D. Hennelly, and T. Deeney, *Inorg. Chim. Acta* **37,** 95 (1979).
13. G. Cao, H. Lee, V. M. Lynch, and T. E. Mallouk, *Solid State Ionics* **26,** 63 (1988).
14. G. Cao, H. Lee, V. M. Lynch, and T. E. Mallouk, *Inorg. Chem.* **27,** 2781 (1988).
15. J. E. Greedan, K. Reubenbauer, T. Birchall, M. Ehlert, D. R. Corbin, and M. A. Subramanian, *J. Solid State Chem.* **77,** 376 (1988).
16. S. G. Carling, P. Day, and D. Visser, *Acta Crystallogr. Sect. A (Suppl.)* **46,** C-278 (1990).
17. D. Visser, S. G. Carling, P. Day, and J. Deportes, *J. Appl. Phys.* **69,** 6016 (1991).
18. J. K. Crockcroft, personal communication.
19. J. S. Rollet, "Computing in Crystallography," Vol. 32, Pergamon, Oxford (1965).
20. "Landolt-Bornstein Numerical Data and Functional Relationships in Science and Technology, New Series. Group 2. Atomic and Molecular Physics" (K. M. Hellwege and A. M. Hellwege, Eds.). Vol. 2 (E. Koenig, Ed.), Springer-verlag, Berlin/Heidelberg (1966).
21. C. J. O'Connor, *Prog. Inorg. Chem.* **29,** 203 (1982).
22. T. Moriya, *Phys. Rev.* **120,** 91 (1960).
23. R. Navarro, "Magnetic Properties of Layered Transition Metal Compounds" (L. J. deJongh, Ed.), p. 105, Kluwer Academic, Dordrecht (1990).
24. E. F. Bertaut, *Acta Crystallogr. Sect. A* **24,** 217 (1968).